

# LANTERN: TCR-Peptide Binding Prediction via Large Language Model Representations

Cong Qi, Hanzhang Fan, Siqi Jiang, Tianxing Hu, and Wei Zhi

New Jersey Institute of Technology

**Abstract.** Predicting T-cell receptor (TCR) and peptide-major histocompatibility complex (pMHC) interactions is vital for advancing targeted immunotherapies and personalized medicine. However, existing models face challenges due to limited data and the constant emergence of novel epitopes, constraining their predictive accuracy. We propose **LANTERN** (Large lAnguage model-powered TCR-Enhanced Recognition Network), a novel framework that leverages large language models to improve TCR-peptide binding prediction. By integrating protein-specific language model embeddings with SMILES encoding, LANTERN effectively captures intricate peptide attributes, enhancing representation capabilities. This design enables improved generalization, particularly in zero-shot and few-shot learning scenarios. Comparative evaluations against ChemBERTa, TITAN, and NetTCR demonstrate LANTERN’s superior performance in predicting unseen epitopic bindings. Our results underscore LANTERN’s potential to improve TCR-antigen interaction modeling, contributing to the development of personalized immunotherapies and vaccines.

**Keywords:** TCR-pMHC interactions · Large language models · Another keyword.

## 1 Introduction

The interaction between T-cell receptors (TCRs) and antigens is a fundamental aspect of adaptive immunity, enabling the body to identify and respond to pathogens and malignancies [5,18]. Accurate prediction of TCR-antigen interactions is critical for developing effective immunotherapies, such as PD-L1/PD-1 inhibitors and adoptive T-cell therapies [3,34]. These treatments rely on a precise understanding of TCR binding behavior to ensure targeted and personalized immune responses. However, predicting these interactions is highly challenging due to the vast diversity of the TCR repertoire and the peptide-major histocompatibility complexes (pMHCs) they recognize [1,13,33]. This complexity arises from the immense combinatorial diversity in TCR sequences, the genetic variability across individuals, and the rapid mutation rates of pathogens, all of which contribute to dynamic and often unpredictable interaction patterns.

Moreover, existing predictive models frequently struggle to generalize across new epitopes or rare TCR variants, limiting their practical utility in clinical and

therapeutic settings [2]. The challenge is further compounded by the fact that TCR-peptide binding is governed not only by sequence similarity but also by intricate structural and chemical properties that are difficult to capture using conventional sequence-based models. As a result, developing robust computational frameworks capable of effectively modeling TCR-antigen recognition remains an urgent research objective.

To address these limitations, we developed **LANTERN** (Large lAngeage model-powered TCR-Enhanced Recognition Network), a deep learning framework designed to improve TCR-antigen binding prediction by combining advanced pre-training techniques with specialized molecular representations. Inspired by the findings of Weber et al. [37], LANTERN integrates two key innovations: embeddings from protein language models (e.g., ESM) and Simplified Molecular Input Line Entry System (SMILES) encoding. The incorporation of SMILES encoding is particularly notable, as it enables the model to capture detailed structural and chemical attributes of peptide sequences. Since peptides involved in TCR recognition are often short, sequence-based models alone may struggle to capture the critical features that influence binding. By translating these sequences into SMILES representations, LANTERN encodes molecular structure and functional group information, enhancing its ability to model complex TCR-antigen interactions.

## 2 Related Work

T cell receptors (TCRs) are comprised of  $\alpha$  and  $\beta$  chains, with the complementarity-determining region 3 (CDR3) being the crucial factor in antigen recognition [24,28,19]. While both chains contribute to this interaction, the  $\beta$  chain is believed to play a more significant role and is more prevalent in existing data [21,10,30]. In light of this and data limitations, many current models, including ours, prioritize the CDR3 sequence of the  $\beta$  chain as input, aligning with approaches by Weber et al. [37] and Lu et al. [22]. To comprehensively evaluate the performance of our model, we carried out comparative experiments on datasets with different negative sample structures. These negative samples include: (1) biologically validated non-binding TCR-epitope pairs sourced from databases such as IEDB and NetTCR-2.0 [12]; (2) randomly paired TCRs and epitopes obtained from positive samples [12,14,17]; and (3) epitopes sampled for each TCR based on the frequency distribution of epitopes in the positive samples [14,17]. This comprehensive assessment strategy allows us to gain insights into the model’s generalization capabilities under various conditions, thus yielding more reliable insights for TCR-pMHC binding prediction studies.

Given the pivotal role of TCR-pMHC interactions in immune recognition, numerous studies have focused on modeling these interactions. Distance-based methods such as GLIPH [20] and TCRdist [19], predict TCR binding by forming clusters based on TCR similarity and determining their peptide specificity. Furthermore, large experimentally validated TCR-peptide binding databases such as VDJdb [39], IEDB [6], and McPAS [32] offer researchers unique opportuni-

ties to apply deep learning techniques for modeling intricate TCR-pMHC data. Among these efforts, Jurtz et al. [16] proposed a model using a 1D CNN to predict whether a given TCR can recognize a specific peptide, taking the peptide’s amino acid sequence and the CDR3 region of the TCR  $\beta$  chain as inputs. Building on this, Montemurro et al. [26] introduced an enhanced framework called NetTCR-2.0, which leverages a more advanced architecture to handle the complexity arising from variations in TCR length and achieves higher accuracy and better generalization in the prediction stage. Likewise, Sidhom et al. [30] presented a deep learning framework called DeepTCR, which integrates CNN with both unsupervised and supervised learning techniques to model TCR sequences.

However, these models typically face the challenge of relying heavily on large amounts of labeled data. The scarcity of high-quality annotated datasets hinders the effective training of machine learning models, preventing them from fully learning the diversity and complexity of the data. This limitation is particularly evident when encountering previously unseen epitopes, leading to insufficient generalization ability and, consequently, reduced predictive performance [12,40]. Although recent next-generation sequencing projects have generated substantial amounts of data on TCR sequences and their cognate HLA-peptide complex targets, this data is still insufficient to address the issue of data scarcity in novel epitope prediction [16,23].

Recent advances in self-supervised learning in the field of natural language processing have been remarkable. The BERT model [35,7,31,15], a milestone pre-trained deep bidirectional representation model based on transformers, has demonstrated excellent performance across multiple downstream tasks and has been widely applied to the natural sciences. For example, Wu et al. [38] proposed the TCR-BERT model, which leverages the BERT framework to learn latent representations from unlabeled TCR sequences. Researchers have shown that TCR-BERT exhibits significantly better generalization ability in downstream tasks compared to other methods [25,41,8]. Additionally, Jiang et al. [14] introduced a predictive method called TEINet, which uses two pre-trained encoders to enhance the model’s ability to learn features from TCR and epitope sequences and accurately predict their binding specificity through transfer learning.

### 3 Methods

#### 3.1 An overview of LANTERN

In this study, we present the LANTERN model, which employs a two-stage deep learning approach using transfer learning to identify patterns in TCR and epitope sequences. In Figure 1, we present a visualization of the LANTERN model. The first stage involves transforming epitope sequences from protein sequences into SMILES sequences to address the issue of short peptide data lengths. Typically, the average protein length is around 10 characters, but after conversion to SMILES, the average length extends to around 185 characters. We begin by tokenizing TCR and epitope sequences into individual characters, which are then processed by their respective pretrained encoders. These encoders convert

character sequences into numerical vectors, producing low-dimensional vector representations. Finally, the encodings of TCRs and epitopes are integrated and fed into a fully connected neural network designed to leverage information from both parts to make accurate predictions.

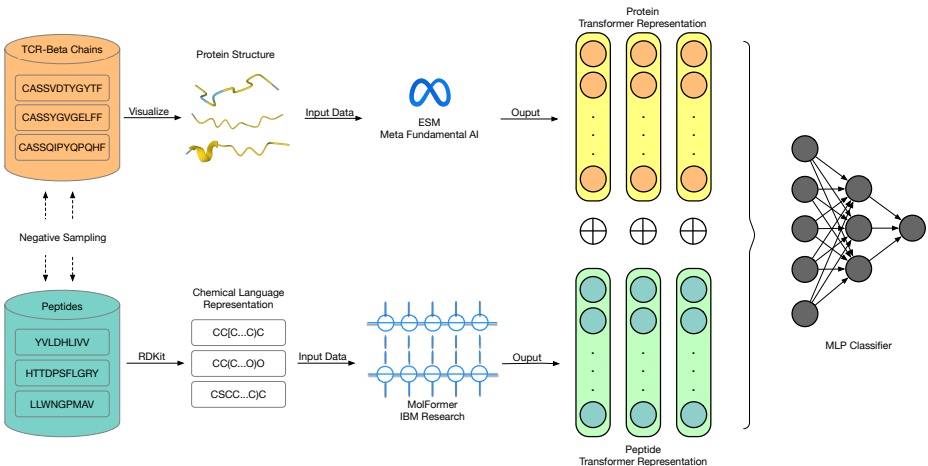


**Fig. 1. Framework of the LANTERN Model** The LANTERN model follows a two-stage deep learning framework utilizing transfer learning. In the first stage, epitope sequences are converted from protein sequences into SMILES representations to address short peptide data lengths. Both TCR and peptide sequences are tokenized and processed through their respective pretrained encoders (ESM for TCRs and MolFormer for peptides), producing numerical vector representations. These embeddings are then concatenated and passed through a fully connected neural network that predicts TCR-peptide binding affinity. This integrated framework effectively captures complex sequence characteristics and enhances performance, particularly in zero-shot and few-shot learning scenarios.

### 3.2 Negative Sampling Strategy

In the context of the TCR-peptide binding problem, two primary strategies are commonly employed for generating negative samples: the reference control and the random control [12].

**Reference Control:** This approach involves negative samples derived from established datasets, providing verified unbound pairs confirmed through biological experiments. While this method offers reliable ground truth data, it is resource-intensive and requires substantial time and experimental effort, posing challenges for large-scale datasets.

**Random Control:** This method generates negative samples by randomly pairing a peptide with a TCR sequence. Although this approach is efficient and requires minimal additional resources, it carries the risk of producing pairs that may still bind, potentially compromising the accuracy of the negative sample set.

Among these strategies, the random control poses a greater challenge due to the possibility of inadvertently generating binding pairs. To ensure the model is evaluated on unseen peptides during testing (i.e., peptides in the test set are absent from the training data), our negative sampling procedure constructs an equal number of negative pairs to match the positive ones in the training set. Specifically, we generate negative samples by randomly pairing one peptide with one TCR from the training data, maintaining the data distribution consistent with the TCHard dataset. Through this process, we generate the corresponding reference control dataset, denoted as Gen NA, and the corresponding random control dataset, denoted as Gen RN. This procedure is formally defined by the following equations:

$$D_{\text{neg}} = \left\{ (TCR_i, Pep_j) \mid \begin{array}{l} TCR_i \in TCR_{\text{train}}, \\ Pep_j \in Pep_{\text{train}}, \\ (TCR_i, Pep_j) \notin D_{\text{pos}} \end{array} \right\}$$

such that  $|D_{\text{neg}}| \propto |D_{\text{pos}}|$

where

- $TCR_{\text{train}}$  is the set of TCR sequences in the training set.
- $Pep_{\text{train}}$  is the set of peptide sequences in the training set.
- $D_{\text{neg}}$  is the set of generated negative samples.
- $D_{\text{pos}}$  is the set of positive samples in the training set.

We prepare data from the TCHard dataset [12] according to the negative sampling strategy. This results in the original reference control dataset (NA), the original random control dataset (RN), the generated reference control dataset (Gen NA), and the generated random control dataset (Gen RN). For all four datasets, we select the TCR Beta chain and the antigen peptide as the input feature, ignoring the TCR Alpha chain, MHC, V, and J genes. This selection is based on findings from the reference paper [9,11,29], which indicates that the Beta chain and antigen peptide are the most critical components for predicting TCR-peptide interactions. By focusing on these elements, we aim to improve prediction accuracy while simplifying the model by excluding less impactful features. We employ a 5-fold split strategy, ensuring that in each split, the original test set from TCHard is used consistently across experiments, and for the original training set, we further split it into a new training set and a validation set in an 8:2 ratio. Throughout all datasets, we maintain a "hard split" methodology, ensuring that peptides in the test or validation set are never seen in the training set. Totally, there are 160,000 TCR beta chains, and 1,000 peptides, resulting in 220,000 TCR-Peptide pairs in the train set, 60,000 validation set and 40,000

TCR-Peptide pairs in the test set. For the detailed statistics, please refer to the Supplementary Data Table 1 and Table 2.

### 3.3 Encoder of TCR and Peptides

The ESM model, a state-of-the-art transformer-based model, is employed for extracting rich, contextual embeddings from protein sequences. ESM’s architecture enables capturing nuanced sequence dependencies and structural motifs critical for protein function, thereby enhancing the understanding of sequence-activity relationships. The model encodes protein sequences into high-dimensional vectors, encapsulating their inherent biological properties. In our framework, this process is mathematically defined as:

$$E_{\text{protein}} = f_{\text{ESM}}(S_{\text{protein}}) = \text{FFN}(\text{LN}(X + \text{MHSA}(\text{LN}(X)))) \quad (1)$$

Breaking this down further, the multi-head self-attention mechanism is given by:

$$\text{MHSA}(X) = \text{Concat}(\text{head}_1, \text{head}_2, \dots, \text{head}_h)W^O \quad (2)$$

where each attention head is computed as:

$$\text{head}_i = \text{Softmax}\left(\frac{Q_i K_i^T}{\sqrt{d_k}}\right) V_i \quad (3)$$

with  $Q_i = XW_i^Q$ ,  $K_i = XW_i^K$ , and  $V_i = XW_i^V$  representing query, key, and value projections for the  $i$ -th attention head.  $W^O$  is the output projection matrix, and  $d_k$  is the dimensionality of the key vectors.

The feed-forward network (FFN) is defined as:

$$\text{FFN}(x) = \text{ReLU}(xW_1 + b_1)W_2 + b_2 \quad (4)$$

where  $W_1$ ,  $W_2$ ,  $b_1$ , and  $b_2$  are learnable parameters.

Simultaneously, MolFormer, a transformer model specifically designed for chemical informatics, encodes small molecules into embeddings that reflect their chemical characteristics and interaction potential with proteins. This model effectively handles diverse and complex chemical structures, transforming them into features conducive to interaction analysis. The embedding process for a peptide  $P$  is described as follows:

$$P_{\text{molecule}} = \text{Convert\_fn}(P_{\text{peptide}}) = \text{DFS}(P_{\text{peptide}}) \quad (5)$$

where DFS represents a Deep First Search algorithm that converts peptide sequences into SMILES representation.

Next, the converted sequence is encoded through the MolFormer model:

$$E_{\text{molecule}} = f_{\text{MolFormer}}(P_{\text{molecule}}) = \text{FFN}(\text{LN}(Y + \text{MHSA}(\text{LN}(Y)))) \quad (6)$$

The embeddings from ESM-1b and MolFormer are subsequently fed into a neural network to predict the binding affinity between the two entities. The prediction model correlates features from both embeddings to infer their binding affinity:

$$BA = f_{MLP}([E_{\text{protein}}, E_{\text{molecule}}]) \quad (7)$$

where  $BA$  denotes the predicted binding affinity obtained from the multi-layer perceptron  $f_{MLP}$ . The MLP itself is defined as:

$$BA = \sigma(W_{MLP}[E_{\text{protein}}, E_{\text{molecule}}] + b_{MLP}) \quad (8)$$

where  $W_{MLP}$  and  $b_{MLP}$  are learnable parameters, and  $\sigma$  is the sigmoid function ensuring the output is within the range  $[0,1]$ .

### 3.4 Objective Function

To further refine this model for binary classification (bind or non-bind prediction), we define the objective function using a binary cross-entropy loss:

$$\mathcal{L} = -\frac{1}{N} \sum_{i=1}^N y_i \log(\hat{y}_i) + (1 - y_i) \log(1 - \hat{y}_i) \quad (9)$$

where  $y_i \in \{0, 1\}$  denotes the ground-truth label for the  $i$ -th sample (1 for binding, 0 for non-binding), and  $\hat{y}_i = \sigma(BA_i)$  represents the predicted probability for the corresponding sample using the sigmoid activation function  $\sigma(x) = \frac{1}{1+e^{-x}}$ .

The model’s performance is rigorously validated against a held-out test set, employing metrics such as AUC-ROC to quantify prediction accuracy and reliability. This methodology of LANTERN, integrating the powerful ESM-1b and MolFormer models, sets the stage for profound advancements in understanding and predicting the dynamics of protein-ligand interactions, with significant implications for drug discovery and biochemical research.

## 4 Experiments

### 4.1 Benchmark Evaluation of LANTERN

The objective is to predict whether the TCR and peptide bind with each other. In LANTERN, we choose Molformer as the peptide SMILES pretraining model and use other state-of-the-art models as baselines for performance comparison. These include Large Language Model-based approaches, including Smiles-Bert [36], TEINet [14], and ChemBERTa [4], as well as end-to-end deep learning models such as TITAN [37], ERGO II [33], NetTCR [26], DlpTcr [42], and Imrex [27]. The main results and analysis demonstrate the powerful performance of Large Language Models in zero-shot learning, effectively capturing the interaction between TCR and peptide. Additionally, their few-shot learning capabilities

highlight their ability to remember and generalize knowledge from other domains to the binding prediction problem.

## 4.2 Performance of LANTERN Compared to Baseline Models

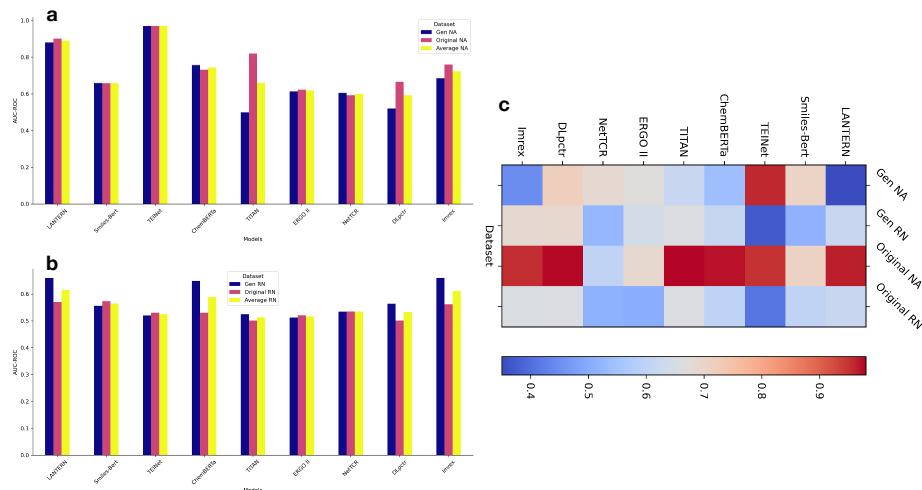


**Fig. 2. Performance of LANTERN on four datasets.** | **a.** AUC-ROC scores across models for NA dataset. **b.** AUC-ROC scores across models for RN dataset. **c.** Accuracy scores across models for the four datasets.

LANTERN exhibits significant improvement over traditional methods. Our experiments highlighted the performance of the LANTERN framework, particularly in the context of the random control setting. Figure 2 presents the AUC-ROC score across the four settings, for the detailed results of all metrics, please refer to the Supplementary Data Table 3 to Table 6. We use six metrics to evaluate performance: AUC-ROC, Accuracy, Recall, Precision, F1-Score, and AUC-PR. Among these, we primarily focus on AUC-ROC, as it is robust to threshold values in binary classification tasks.

Additionally, the LANTERN model demonstrates robust performance, significantly outperforming baseline methods, which are reflected in the following three key observations. Specifically, Large Language Models (LLMs) consistently outperforms end-to-end deep learning models. The mean AUC-ROC score for LLM-based models of 0.8165, compared to 0.5846 for deep learning models, showing an average increase of 0.2319 for LLM-based models. Specifically, LANTERN achieved an AUC-ROC score of 0.88 on Gen NA, significantly higher than many other models. This demonstrates the superior capability of LLM-based models in

capturing complex interactions between TCR and peptides. The success of LLM-based models can be attributed to their ability to leverage extensive pretraining on diverse datasets, enabling them to generalize effectively to new, unseen data. This zero-shot learning capability allows these models to recognize patterns and relationships that end-to-end models may miss without extensive retraining.

**Comparison of Generated vs. Original Datasets** Comparing results between Gen NA (Supplementary Data Table 3) and Original NA (Supplementary Data Table 5), and Gen RN (Supplementary Data Table 4) and Original RN (Supplementary Data Table 6) reveal that models trained on generated datasets generally performed better than those trained on original datasets. For instance, LANTERN achieves an AUC-ROC score of 0.88 on Gen NA versus 0.901 on Original NA, and 0.66 on Gen RN versus 0.57 on Original RN. This suggests that the novel negative sample generation method improved model training by providing more realistic and challenging scenarios, closely mimicking the complexities of real-world data. The generation of negative samples in Gen NA and Gen RN datasets allowed for a more balanced and comprehensive training process. This method ensures that the model encounters a variety of binding and non-binding interactions, enhancing its ability to distinguish between them. By incorporating a diverse range of negative samples, the model becomes more adept at recognizing subtle differences in binding patterns, leading to improved prediction accuracy and robustness.

**Generally Challengeable Random Control Setting** Although LANTERN showed higher performance over the random control setting, there is still room for improvement, as the AUC-ROC score of 0.66 is relatively low. The random control setting is more challenging than the reference control setting due to its nature of generating negative samples quickly and resource-efficiently. However, it requires further exploration to enhance robustness and address this challenge effectively. The random control setting presents unique challenges due to the inherent variability and randomness of the generated negative samples. While this approach is efficient and scalable, it can introduce noise and ambiguity into the training process. To address these challenges, future research could explore advanced techniques for negative sample generation, such as leveraging domain-specific knowledge or incorporating additional biological context to improve the quality and relevance of the negative samples. Additionally, integrating ensemble learning methods or incorporating multimodal data sources could further enhance the model’s performance and generalization capabilities.

**Embedding Cluster of Pretraining Model** To visualize the impact of using pretraining models on our embeddings, we clustered the TCR and antigen embeddings generated by LANTERN with and without the utilization of ESM and MolFormer pretraining. The Hopkins score for the pretraining model is 0.90, and the Cluster Tendency Score (CTS) is 0.86. Specifically, we sampled 10,000

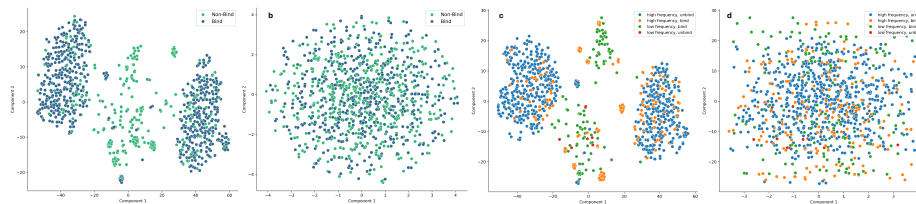


**Fig. 3. t-SNE visualization of the embeddings from LANTERN model. | a.** With pretrain of 0.857 h score. **b.** Without pretrain of 0.607 h score. **c.** Show frequency of the pretrained embeddings. **d.** Show frequency of the no pretrained embeddings.

embeddings from the pretrained model and reset the labels to the ground truth of binding or unbinding. Using the t-SNE method to reduce the dimensions to a 2D plane, we obtained the clusters shown in Figure 3.

From Figure 3a and 3b, it is evident that there is a clear boundary between the two classes (bind and non-bind), making it easier for the classifier to distinguish between them. This separation illustrates the effectiveness of the pretraining in enhancing the clustering of embeddings, thus aiding the model’s classification performance. Additionally, we evaluated whether the pretrained embeddings could reflect the property of low and high frequency. We mapped the low/high frequency to the first dimension, resulting in four classes: [low frequency, unbind], [low frequency, bind], [high frequency, unbind], and [high frequency, bind], as shown in Figure 3c and 3d. The figures show that the model can also distinguish between high and low frequencies effectively. These visualizations demonstrate that the pretrained embeddings not only provide clear separations between binding and non-binding classes but also accurately reflect the frequency characteristics, further supporting the robustness and effectiveness of the pretraining approach in our model.

### Quantitative Evaluation of Embedding Performance

**Embedding Cluster of Pretraining Model** To further quantify the performance of the embeddings learned by the pretraining model, we calculated several clustering performance metrics: Silhouette Index (SI) and Calinski-Harabasz Index (CHI). Additionally, we evaluated unsupervised metrics, including the Hopkins Score (HS) and Cluster Tendency Score (CTS) [43]. For SI and CH, we employed the K-means clustering method on the embeddings with  $k = 2$ . We put the algorithm for these metrics in the supplementary section 2. The results are illustrated in the Figure 4. In Figure 4, we observe the following metrics:

- **Cluster Tendency Score (CTS):** With pretraining, CTS achieved a score of 0.96, significantly higher than the 0.41 score without pretraining. This indicates that the pretraining model substantially improves the clustering tendency of the embeddings.

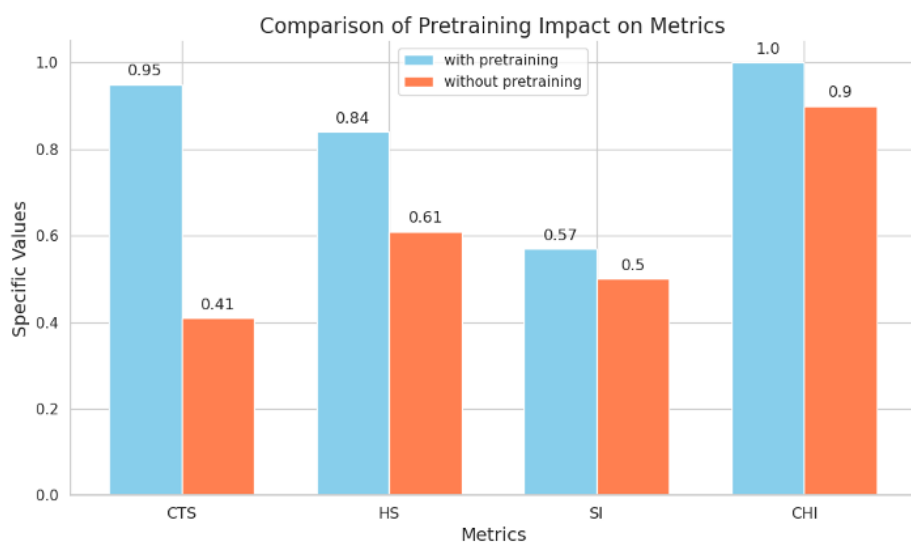


**Fig. 4.** Comparison of cluster metrics between embeddings with or without pretraining. The SI and CHI scores are scaled by sigmoid function to make them more readable.

- Hopkins Score (HS): The Hopkins Score with pretraining is 0.84, compared to 0.61 without pretraining. A higher Hopkins Score suggests better cluster formation, reinforcing the effectiveness of pretraining.
- Silhouette Index (SI): The SI score is 0.31 with pretraining and 0.00 without pretraining, demonstrating better-defined clusters with pretraining.
- Calinski-Harabasz Index (CHI): The CHI with pretraining is 1. (scaled from 389.06), dramatically higher than the 0.9 (scaled from 2.12) without pretraining, indicating that the embeddings with pretraining result in more compact and well-separated clusters.

These metrics collectively illustrate the advantage of using LANTERN with pretraining. The significant improvements in CTS, HS, SI, and CHI scores indicate that the pretraining enhances the quality of the embeddings, leading to better-defined and more distinguishable clusters. This improved clustering performance directly contributes to the model’s ability to accurately predict TCR-peptide interactions, showcasing the robustness and effectiveness of the pretraining approach.

### 4.3 Few-Shot Learning Capabilities of LANTERN

Previous sections highlighted the powerful performance of LANTERN in zero-shot learning settings. Next, we explore the model’s performance in few-shot learning scenarios. The few-shot learning capabilities of LLM-based models en-

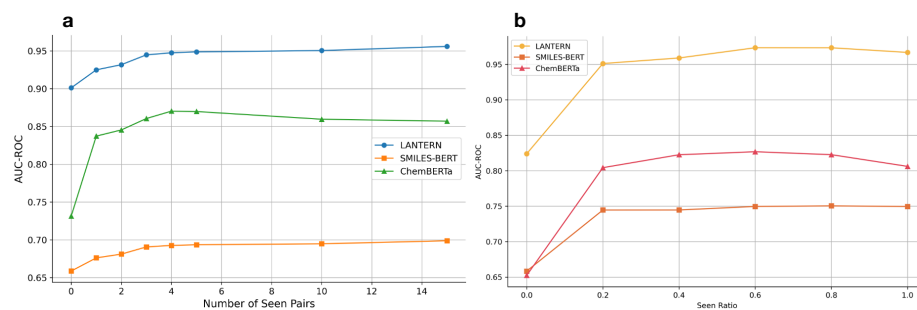


**Fig. 5. Few-Shot Learning performance of LANTERN** | a. Performance comparison of models over different numbers of seen pairs. b. Performance comparison of models over different seen ratios.

able them to adapt quickly to new tasks with minimal additional training data, demonstrating their flexibility and robustness in various contexts. Few-shot learning is a more common setting encountered in practice. It involves training the model with only a limited number of samples (5 or fewer) of TCR and peptide pairs, aiming to achieve better performance from these limited samples. If the model can learn effectively from a few samples, it becomes significantly more useful in real-world applications. To introduce the few-shot learning setting, we control two variables: the number of peptides seen by the training set and the number of TCR-peptide pairs for each seen peptide in the training set. By carefully managing these variables, we can evaluate LANTERN’s ability to generalize and perform well with minimal data, which is crucial for practical applications where data is often scarce.

In Figure 5a, we maintain 20% seen ratio for the peptide in the training set and test set, then we gradually increase the number of TCR-Peptide pairs for each peptide in the training set. The result suggests two points: 1. the performance of LANTERN and baseline models shows a rapid increase with only a few peptide-TCR pairs (fewer than 5) in the training set. This is particularly beneficial as it indicates that even with limited experimental data, the model can effectively understand the binding or non-binding information of the peptide, reducing the need for extensive data. 2. The performance increase speed is gradually slow when the TCR-Peptide pairs increase, this trend suggests that the model reaches saturation to the seen data, if we want to further improve the performance, we should add more and more data to the model. This also indirectly supports the scaling law.

In Figure 5b, we control the number of TCR-Peptide pairs, limiting it to 5 pairs for each peptide in the training set, and gradually increase the ratio of seen peptides in the training set. The results indicate that as the seen ratio increases, the performance of the models improves steadily. Specifically, the MoleFormer

model shows a steep increase in AUC-ROC as the seen ratio rises, reaching near-perfect accuracy when the seen ratio is at its maximum. This trend suggests that MoleFormer is highly effective at predicting with increasing exposure to seen peptides, achieving almost 100% accuracy under a fully seen setting. In contrast, SMILES-BERT and ChemBERTa demonstrate more modest improvements, with SMILES-BERT showing the least sensitivity to the increasing seen ratio, plateauing at a lower AUC-ROC compared to the other models.

## 5 Discussion and Conclusion

The LANTERN model presents a significant advancement in the field of T-cell receptor (TCR) and peptide-major histocompatibility complex (pMHC) binding prediction, leveraging large language model (LLM) representations to address limitations in current methodologies. The integration of pre-trained embeddings from protein language models and SMILES encoding of peptides provides a nuanced understanding of TCR-pMHC interactions, which has been demonstrated through the model’s ability to perform well in both zero-shot and few-shot learning scenarios. This capability is particularly important in the context of predicting previously unseen epitopes, a key challenge for existing models.

One of the critical strengths of LANTERN is its ability to generalize from minimal data, effectively tackling the issue of data scarcity that plagues many deep learning approaches in immunogenetics. The performance of LANTERN across different negative sampling strategies, particularly in the random control setting, illustrates its robustness and versatility. The model consistently outperformed baseline methods, including traditional deep learning and other LLM-based models, across multiple evaluation metrics such as AUC-ROC, precision, and recall. This indicates that the LANTERN framework captures more complex binding patterns compared to other methods, providing a more accurate and reliable prediction of TCR-pMHC interactions.

However, there is still room for improvement, especially in the random control setting, where the performance, while strong, did not reach the same levels as in the reference control setting. This suggests that further refinement of the negative sample generation process, perhaps incorporating domain-specific knowledge or more sophisticated biological features, could enhance the model’s ability to distinguish between true negative and binding pairs. Future work could explore the use of ensemble learning techniques or the incorporation of multimodal data, such as structural or contextual biological information, to improve the model’s performance further.

In conclusion, LANTERN represents a notable step forward in the field of TCR-pMHC binding prediction. Its ability to generalize across novel epitopes and its strong performance in low-data environments make it a valuable tool for advancing personalized immunotherapies and vaccines. Future research will likely focus on enhancing its robustness and exploring additional biological contexts to push the boundaries of what is possible in TCR-pMHC interaction prediction.

**Acknowledgments.** We would like to express our gratitude to our collaborators for their insightful discussions and technical support throughout this work.

**Disclosure of Interests.** The authors have no competing interests to declare that are relevant to the content of this article.

## References

1. Cai, M., Bang, S., Zhang, P., Lee, H.: Atm-tcr: Tcr-epitope binding affinity prediction using a multi-head self-attention model. *Frontiers in immunology* **13**, 893247 (2022)
2. Castorina, L.V., Grazioli, F., Machart, P., Mösch, A., Errica, F.: Assessing the generalization capabilities of tcr binding predictors via peptide distance analysis. *bioRxiv* pp. 2023–07 (2023)
3. Chen, R.Y., Zhu, Y., Shen, Y.Y., Xu, Q.Y., Tang, H.Y., Cui, N.X., Jiang, L., Dai, X.M., Chen, W.Q., Lin, Q., et al.: The role of pd-1 signaling in health and immune-related diseases. *Frontiers in Immunology* **14**, 1163633 (2023)
4. Chithrananda, S., Grand, G., Ramsundar, B.: Chemberta: large-scale self-supervised pretraining for molecular property prediction. *arXiv preprint arXiv:2010.09885* (2020)
5. Davis, M.M., Bjorkman, P.J.: T-cell antigen receptor genes and t-cell recognition. *Nature* **334**(6181), 395–402 (1988)
6. De Neuter, N., Bittremieux, W., Beirnaert, C., Cuypers, B., Mrzic, A., Moris, P., Suls, A., Van Tendeloo, V., Ogunjimi, B., Laukens, K., et al.: On the feasibility of mining cd8+ t cell receptor patterns underlying immunogenic peptide recognition. *Immunogenetics* **70**, 159–168 (2018)
7. Devlin, J., Chang, M.W., Lee, K., Toutanova, K.: Bert: Pre-training of deep bidirectional transformers for language understanding. In: *Proceedings of the 2019 conference of the North American chapter of the association for computational linguistics: human language technologies, volume 1 (long and short papers)*. pp. 4171–4186 (2019)
8. Fan, T., Zhang, M., Yang, J., Zhu, Z., Cao, W., Dong, C.: Therapeutic cancer vaccines: advancements, challenges and prospects. *Signal Transduction and Targeted Therapy* **8**(1), 450 (2023)
9. Feng, D., Bond, C.J., Ely, L.K., Maynard, J., Garcia, K.C.: Structural evidence for a germline-encoded t cell receptor–major histocompatibility complex interaction ‘codon’. *Nature immunology* **8**(9), 975–983 (2007)
10. Fidelle, M., Rauber, C., Alves Costa Silva, C., Tian, A.L., Lahmar, I., de La Varenne, A.L.M., Zhao, L., Thelemaque, C., Lebhhar, I., Messaoudene, M., et al.: A microbiota-modulated checkpoint directs immunosuppressive intestinal t cells into cancers. *Science* **380**(6649), eabo2296 (2023)
11. Glanville, J., Huang, H., Nau, A., Hatton, O., Wagar, L.E., Rubelt, F., Ji, X., Han, A., Krams, S.M., Pettus, C., et al.: Identifying specificity groups in the t cell receptor repertoire. *Nature* **547**(7661), 94–98 (2017)
12. Grazioli, F., Mösch, A., Machart, P., Li, K., Alqassem, I., O’Donnell, T.J., Min, M.R.: On tcr binding predictors failing to generalize to unseen peptides. *Frontiers in immunology* **13**, 1014256 (2022)
13. Heumos, L., Schaar, A.C., Lance, C., Litinetskaya, A., Drost, F., Zappia, L., Lücken, M.D., Strobl, D.C., Henao, J., Curion, F., et al.: Best practices for single-cell analysis across modalities. *Nature Reviews Genetics* **24**(8), 550–572 (2023)

14. Jiang, Y., Huo, M., Cheng Li, S.: Teinet: a deep learning framework for prediction of tcr-epitope binding specificity. *Briefings in bioinformatics* **24**(2), bbad086 (2023)
15. Jin, M., Wang, S., Ma, L., Chu, Z., Zhang, J.Y., Shi, X., Chen, P.Y., Liang, Y., Li, Y.F., Pan, S., et al.: Time-llm: Time series forecasting by reprogramming large language models. arXiv preprint arXiv:2310.01728 (2023)
16. Jurtz, V.I., Jessen, L.E., Bentzen, A.K., Jespersen, M.C., Mahajan, S., Vita, R., Jensen, K.K., Marcatili, P., Hadrup, S.R., Peters, B., et al.: Nettcr: sequence-based prediction of tcr binding to peptide-mhc complexes using convolutional neural networks. *BioRxiv* p. 433706 (2018)
17. Korpela, D., Jokinen, E., Dumitrescu, A., Huuhtanen, J., Mustjoki, S., Lähdesmäki, H.: Epic-trace: predicting tcr binding to unseen epitopes using attention and contextualized embeddings. *Bioinformatics* **39**(12), btad743 (2023)
18. Krogsgaard, M., Davis, M.M.: How t cells' see'antigen. *Nature immunology* **6**(3), 239–245 (2005)
19. La Gruta, N.L., Gras, S., Daley, S.R., Thomas, P.G., Rossjohn, J.: Understanding the drivers of mhc restriction of t cell receptors. *Nature Reviews Immunology* **18**(7), 467–478 (2018)
20. Lin, Z., Akin, H., Rao, R., Hie, B., Zhu, Z., Lu, W., dos Santos Costa, A., Fazel-Zarandi, M., Sercu, T., Candido, S., et al.: Language models of protein sequences at the scale of evolution enable accurate structure prediction. *BioRxiv* **2022**, 500902 (2022)
21. Lipkova, J., Chen, R.J., Chen, B., Lu, M.Y., Barbieri, M., Shao, D., Vaidya, A.J., Chen, C., Zhuang, L., Williamson, D.F., et al.: Artificial intelligence for multimodal data integration in oncology. *Cancer cell* **40**(10), 1095–1110 (2022)
22. Lu, T., Zhang, Z., Zhu, J., Wang, Y., Jiang, P., Xiao, X., Bernatchez, C., Heymach, J.V., Gibbons, D.L., Wang, J., et al.: Deep learning-based prediction of the t cell receptor-antigen binding specificity. *Nature machine intelligence* **3**(10), 864–875 (2021)
23. Lybaert, L., Lefever, S., Fant, B., Smits, E., De Geest, B., Breckpot, K., Dirix, L., Feldman, S.A., Van Criekinge, W., Thielemans, K., et al.: Challenges in neoantigen-directed therapeutics. *Cancer Cell* **41**(1), 15–40 (2023)
24. Mayassi, T., Barreiro, L.B., Rossjohn, J., Jabri, B.: A multilayered immune system through the lens of unconventional t cells. *Nature* **595**(7868), 501–510 (2021)
25. Mhanna, V., Bashour, H., Lê Quỳ, K., Barennes, P., Rawat, P., Greiff, V., Mariotti-Ferrandiz, E.: Adaptive immune receptor repertoire analysis. *Nature Reviews Methods Primers* **4**(1), 6 (2024)
26. Montemurro, A., Schuster, V., Povlsen, H.R., Bentzen, A.K., Jurtz, V., Chronister, W.D., Crinklaw, A., Hadrup, S.R., Winther, O., Peters, B., et al.: Nettcr-2.0 enables accurate prediction of tcr-peptide binding by using paired tcr $\alpha$  and  $\beta$  sequence data. *Communications biology* **4**(1), 1060 (2021)
27. Moris, P., De Pauw, J., Postovskaya, A., Gielis, S., De Neuter, N., Bittremieux, W., Ogunjimi, B., Laukens, K., Meysman, P.: Current challenges for unseen-epitope tcr interaction prediction and a new perspective derived from image classification. *Briefings in bioinformatics* **22**(4), bbaa318 (2021)
28. Pai, J.A., Satpathy, A.T.: High-throughput and single-cell t cell receptor sequencing technologies. *Nature methods* **18**(8), 881–892 (2021)
29. Rowen, L., Koop, B.F., Hood, L.: The complete 685-kilobase dna sequence of the human  $\beta$  t cell receptor locus. *Science* **272**(5269), 1755–1762 (1996)
30. Sidhom, J.W., Larman, H.B., Pardoll, D.M., Baras, A.S.: Deeptcr is a deep learning framework for revealing sequence concepts within t-cell repertoires. *Nature communications* **12**(1), 1605 (2021)

31. Singhal, K., Azizi, S., Tu, T., Mahdavi, S.S., Wei, J., Chung, H.W., Scales, N., Tanwani, A., Cole-Lewis, H., Pfohl, S., et al.: Large language models encode clinical knowledge. *Nature* **620**(7972), 172–180 (2023)
32. Smith-Garvin, J.E., Koretzky, G.A., Jordan, M.S.: T cell activation. *Annual review of immunology* **27**(1), 591–619 (2009)
33. Springer, I., Tickotsky, N., Louzoun, Y.: Contribution of t cell receptor alpha and beta cdr3, mhc typing, v and j genes to peptide binding prediction. *Frontiers in immunology* **12**, 664514 (2021)
34. Tang, Q., Chen, Y., Li, X., Long, S., Shi, Y., Yu, Y., Wu, W., Han, L., Wang, S.: The role of pd-1/pd-l1 and application of immune-checkpoint inhibitors in human cancers. *Frontiers in immunology* **13**, 964442 (2022)
35. Vaswani, A., Shazeer, N., Parmar, N., Uszkoreit, J., Jones, L., Gomez, A.N., Kaiser, Ł., Polosukhin, I.: Attention is all you need. *Advances in neural information processing systems* **30** (2017)
36. Wang, S., Guo, Y., Wang, Y., Sun, H., Huang, J.: Smiles-bert: large scale unsupervised pre-training for molecular property prediction. In: *Proceedings of the 10th ACM international conference on bioinformatics, computational biology and health informatics*. pp. 429–436 (2019)
37. Weber, A., Born, J., Rodriguez Martínez, M.: Titan: T-cell receptor specificity prediction with bimodal attention networks. *Bioinformatics* **37**(Supplement\_1), i237–i244 (2021)
38. Wu, K.E., Yost, K., Daniel, B., Belk, J., Xia, Y., Egawa, T., Satpathy, A., Chang, H., Zou, J.: Tcr-bert: learning the grammar of t-cell receptors for flexible antigen-binding analyses. In: *Machine Learning in Computational Biology*. pp. 194–229. PMLR (2024)
39. Wu, R., Ding, F., Wang, R., Shen, R., Zhang, X., Luo, S., Su, C., Wu, Z., Xie, Q., Berger, B., et al.: High-resolution de novo structure prediction from primary sequence. *BioRxiv* pp. 2022–07 (2022)
40. Xie, N., Shen, G., Gao, W., Huang, Z., Huang, C., Fu, L.: Neoantigens: promising targets for cancer therapy. *Signal transduction and targeted therapy* **8**(1), 9 (2023)
41. Xu, Y., Liu, X., Cao, X., Huang, C., Liu, E., Qian, S., Liu, X., Wu, Y., Dong, F., Qiu, C.W., et al.: Artificial intelligence: A powerful paradigm for scientific research. *The Innovation* **2**(4) (2021)
42. Xu, Z., Luo, M., Lin, W., Xue, G., Wang, P., Jin, X., Xu, C., Zhou, W., Cai, Y., Yang, W., et al.: Dlptcr: an ensemble deep learning framework for predicting immunogenic peptide recognized by t cell receptor. *Briefings in Bioinformatics* **22**(6), bbab335 (2021)
43. Zheng, G., Rymuza, J., Gharavi, E., LeRoy, N.J., Zhang, A., Sheffield, N.C.: Methods for evaluating unsupervised vector representations of genomic regions. *NAR Genomics and Bioinformatics* **6**(3), lqae086 (2024)